

Comparative Analysis of MFO, GWO and GSO for Classification of Covid-19 Chest X-Ray Images

Asraa M.Mohammad¹, Hussien Attia², Yossra H. Ali³

¹Department of Computer Sciences, College of Science for Women, University of Babylon, Babylon, Iraq.

²Computer sciences department, College of Science for Women, University of Babylon, Iraq.

³Department of Computer sciences, University of Technology, Baghdad, Iraq.

*Corresponding Author.

Received 11/06/2023, Revised 21/08/2023, Accepted 23/08/2023, Published 30/08/2023



This work is licensed under a [Creative Commons Attribution 4.0 International License](https://creativecommons.org/licenses/by/4.0/).

Abstract

Medical images play a crucial role in the classification of various diseases and conditions. One of the imaging modalities is X-rays which provide valuable visual information that helps in the identification and characterization of various medical conditions. Chest radiograph (CXR) images have long been used to examine and monitor numerous lung disorders, such as tuberculosis, pneumonia, atelectasis, and hernia. COVID-19 detection can be accomplished using CXR images as well. COVID-19, a virus that causes infections in the lungs and the airways of the upper respiratory tract, was first discovered in 2019 in Wuhan Province, China, and has since been thought to cause substantial airway damage, badly impacting the lungs of affected persons. The virus was swiftly gone viral around the world and a lot of fatalities and cases growing were recorded on a daily basis. CXR can be used to monitor the effects of COVID-19 on lung tissue. This study examines a comparison analysis of k-nearest neighbors (KNN), Extreme Gradient Boosting (XGboost), and Support-Vector Machine (SVM) are some classification approaches for feature selection in this domain using The Moth-Flame Optimization algorithm (MFO), The Grey Wolf Optimizer algorithm (GWO), and The Glowworm Swarm Optimization algorithm (GSO). For this study, researchers employed a data set consisting of two sets as follows: 9,544 2D X-ray images, which were classified into two sets utilizing validated tests: 5,500 images of healthy lungs and 4,044 images of lungs with COVID-19. The second set includes 800 images, 400 of healthy lungs and 400 of lungs affected with COVID-19. Each image has been resized to 200x200 pixels. Precision, recall, and the F1-score were among the quantitative evaluation criteria used in this study.

Keywords: Classification, COVID-19, extreme gradient boosting, Moth-Flame Optimization algorithm (MFO), Grey Wolf Optimizer algorithm (GWO), Glowworm Swarm Optimization algorithm (GSO).

Introduction

COVID-19 is a highly contagious virus that can spread through the air and survive on surfaces for up to 48 hours. The virus originated in Wuhan, China, and was initially referred to as the Wuhan virus ¹. It rapidly evolved into a global pandemic, affecting people worldwide in a detrimental

manner. Recognizing its severity, the World Health Organization (WHO) declared it a worldwide health emergency in January 2020. Infected individuals may develop symptoms, and the virus can spread in various situations. The incubation period can range from two days to two weeks. Common signs and

symptoms include high body temperature, difficulty breathing, coughing, chest discomfort, loss of smell or taste, nausea, vomiting, headache, and fatigue^{2,3}.

The COVID-19 pandemic put an immense strain on healthcare systems worldwide, leading to a shortage of hospital beds and healthcare professionals. Frontline healthcare workers, including physicians, nurses, and caregivers, faced heightened vulnerability. Timely detection of pneumonia played a crucial role in containing the outbreak through patient quarantining and effective treatment⁴. In this context, computer-aided diagnosis using chest X-rays significantly improved the efficiency of diagnosing pneumonia⁵. However, the diagnosis of medical imaging like X-ray scans can be exceptionally challenging due to the presence of noise and artifacts.

The integration of artificial intelligence (AI) has gained traction, especially in the healthcare sector, owing to its remarkable data processing capabilities, surpassing human capabilities. Consequently, there is a growing demand for automated systems with well-established methodologies for disease detection and diagnosis, considering the escalating number of COVID-19 cases worldwide⁶.

The effectiveness of disease diagnosis using AI-based methods has been demonstrated, underscoring the necessity for such automated systems⁷.

Recently, a novel detection approach employing the Swarm Intelligence algorithm has shown promising results. These algorithms can efficiently process large datasets and extract meaningful patterns and features from medical images, such as chest X-rays, even in the presence

of noise and artifacts. The Swarm Intelligence algorithm's ability to explore a wide range of solutions and converge on the best possible outcome makes it highly effective in optimizing disease detection models. The paper proposes a comparative analysis system that incorporates three optimization algorithms (GSO, GWO, MFO) to address feature selection issues and conduct a comprehensive analysis.

In this context, this study aims to explore the potential of the Swarm Intelligence algorithm in disease detection, particularly in the context of COVID-19. By employing optimization algorithms such as GSO, GWO, and MFO, the proposed comparative analysis system seeks to enhance the accuracy and efficiency of disease diagnosis using chest X-ray images. These optimization algorithms work collaboratively to select relevant features from the images, enhancing the diagnostic capabilities of the automated system. By leveraging the collective intelligence of these algorithms, medical professionals can benefit from more precise and timely disease detection, enabling better patient care and management.

Overall, the integration of AI and Swarm Intelligence algorithms holds significant promise for advancing medical diagnosis and tackling the challenges posed by infectious diseases like COVID-19. This research contributes to the ongoing efforts to develop automated systems capable of accurately detecting and diagnosing diseases, benefiting healthcare professionals and patients alike, the study aims to achieve this goal, and Fig. 1 illustrates the proposed comparative analysis system's steps.

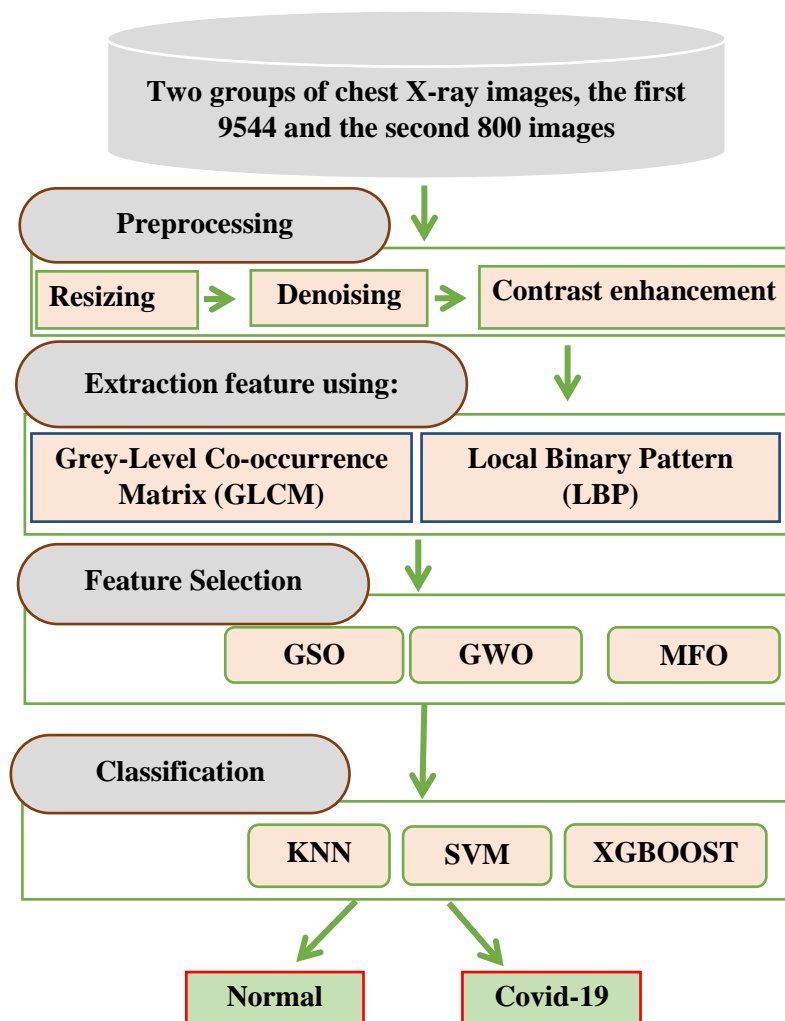


Figure 1. The proposed system of comparative analysis

Related Works

Swarm algorithms have recently been widely used by scholars to address a variety of problems, notably in the optimization of feature selection. Swarm algorithms are currently attracting a lot of interest.

Research employing a particle swarm algorithm and a support vector machine classifier to detect cases of COVID-19 was published in 2020 by Suhaila N. Mohammed et al. ⁸. Patients with COVID-19 have been investigated by studying their CT scans.

For selecting features using a binary dragonfly algorithm, Jingwei Too and Seydali

Mirjalili ⁹ described a novel technique for wrapper-based COVID-19 detection in 2020. Timea Bezdán et al. ¹⁰ created a feature selection approach in 2021 using the Firefly Algorithm for classifying 21 different data sets. In 2022, an improved version of the Greedy Harris Hawks Optimizer was presented for feature selection by Lewang Zou et al. ¹¹. A greedy strategy was used to improve global search capabilities, and an improved differential perturbation methodology has replaced the previous HHO exploitation technique.

Below is Table 1 Comparing the relevant research.

Table 1. Comparing the relevant research

Reference	Algorithm	Problems	Shortcomings
¹²	HHO, SSA, WOA, GWO	Covid-19 detecting	The amount of features set is limited, and the classification accuracy is below 96%.
⁸	Particle Swarm Optimization (PSO)	Detecting of covid-19	The study employs a limited number of features for the classification
⁹	Dragonfly	Detecting of covid-19	The classification accuracy falls below 94%, and the number of features is limited.
¹⁰	Firefly	Classifying of multiple datasets	The researcher was content with utilizing a single classifier for the classification problem, despite working with numerous datasets
¹¹	HHO	Increasing global search capabilities	In feature selection problem, IGHHO performed better than the other compared algorithms in general, but it did not achieve first-place rankings in most cases.

Swarm Intelligence Algorithms

Swarm Intelligence techniques refer to optimization methods that can efficiently identify the best or close-to-best solution to optimization problems. These algorithms have various advantages, including their straightforwardness, adaptability, and ability to overcome the problem of local optima. These methods involve two significant stages: exploitation and exploration ¹². The algorithms are extensively examine the potential searching region during the exploration stage. During that stage, those algorithms conduct a local search for the most promising region(s) found during the exploration stage

Moth-Flame Optimization algorithm (MFO)

The Moth-Flame Optimization algorithm (MFO) draws inspiration from the navigation strategy of moths and aims to apply this natural phenomenon to the optimization process. Moths, like butterflies, belong to the same family and possess around 160,000 unique species in their natural habitats. During their lifetime, moths go through two main stages: larvae and adulthood. The transformation from larvae to a moth occurs within a cocoon.

The key aspect that MFO emulates from moths is its transverse orientation navigational strategy. Moths have a fascinating ability to maintain their orientation with respect to the moon

while flying at night. This phenomenon, known as "transverse orientation," allows them to cover great distances efficiently by moving in straight lines.

The algorithm utilizes this navigational behavior by considering moths as potential solutions to optimization problems. Each moth represents a candidate solution, and their flight towards the moon (or a source of light, symbolizing the optimum) symbolizes the search for an optimal solution. The intensity of the light source reflects the objective function to be optimized.

At each iteration, the MFO algorithm updates the position of moths based on their current orientation towards the light source. Moths with better fitness, i.e., closer to the optimal solution, attract others to move towards them, mimicking the attraction to brighter regions in the environment. Meanwhile, random movements are also incorporated to ensure diversity and exploration within the search space.

The main objective of the Moth-Flame Optimization algorithm is to iteratively refine the positions of moths until a satisfactory or near-optimal solution is achieved. By imitating the navigational behavior of moths and incorporating attraction to light sources, the algorithm effectively explores the search space and converges towards promising regions that can lead to optimal solutions

for a wide range of optimization problems¹³. Algorithm1 outlines the stages of MFO.

Algorithm1: Moth-Flame Optimization Pseudocode¹³

1. **Input:** The objective function $f(X)$ that the Moth-Flame Optimization algorithm aims to optimize is a fitness function that evaluates the quality of a given solution represented by a set of variables $X = (X_1, X_2, \dots, X_d)$, Number of moths in the population (N), dimension (d), Maximum iteration (Maximumiter), Flame number ($N.FM$), and b are the inputs;
 2. **Output:** optimum ecological choice with the lowest fitness function value
-

3. **For** $i = 1: N$

4. **for** $j = 1: d$

5. Produce solutions for N -organisms using the following equation, $X_{i,j}$ ($i = 1, 2 \dots N$).

(This step initializes the positions of moths in the search space by assigning random values within the lower bound ($LB(i)$) and upper bound ($UB(i)$) for each dimension).

$$X(i, j) = LB(i) + (UB(i) - LB(i)) * rand();$$

($X(i, j)$ represents the position of the i th moth in the j th dimension. $rand()$ generates a random number between 0 and 1).

6. **end for**

7. **end for**

8. fitness value $f(X)$ calculated for each moth in the population:

9. **While** Currentiter < Maximumiter +1

10. **if** Iteration == 1

11. Enter $N.FM = N$ in initial population

12. **else**

 Employ using

$$N.FM = \text{round}(N.FM_{\text{lastiter}} - \text{Currentiter} (N.FM_{\text{lastiter}} - 1) / \text{Maxiter})$$

13. **end if**

14. $FM = \text{Fitness Function } f(x)$;

15. **if** Iteration == 1

16. arrange the moths according to FM

17. Update F_{mi}

18. Iteration = 0;

19. **else**

 moths according to FM from last iteration.

```
20.           Update Fmi
21.           end if
22.           for j = 1: N
23.               for k = 1 : d
24.                   Find r and t using
r = -1+ Current, iter (-1/Maxiter) & t = ( r - 1 )x k + 1
25.                   Update Moths' location in relation to their specific flame.
26.               end for
27.           end if
28.           Current iter = Current iter + 1;
29. end while
```

Grey wolf optimizer algorithm (GWO)

It is an innovative metaheuristic algorithm inspired by the natural behaviors and characteristics of grey wolves. The algorithm utilizes a population-based approach, drawing insights from the cooperative hunting strategies employed by this specific subspecies of wolves.

Grey wolves are known for their high intelligence, adaptability, and social hierarchy. They are skilled at cooperating within their packs to efficiently hunt prey and overcome challenges posed by their environment and enemies. The GWO algorithm emulates these characteristics to tackle optimization problems effectively.

In the GWO algorithm, the population consists of a group of candidate solutions, similar to a wolf pack. Each candidate solution represents a potential solution to the optimization problem. Like the wolves, the algorithm encourages collaboration and information sharing among individuals in the population. During the optimization process, the wolves simulate hunting and exploring behaviors to search for the optimal solution.

At each iteration, the GWO algorithm updates the position of each wolf (candidate solution) based on

its fitness, which reflects its performance in solving the optimization problem. The wolves dynamically adjust their positions using three key actions: encircling prey, attacking, and following the leader. These actions mimic the wolves' real-life hunting strategies.

Encircling prey is akin to the wolves surrounding potential solutions with better fitness, which can improve search space exploration. The attacking action involves focusing on the most promising solutions to intensify the exploitation of the search space. Following the leader imitates the wolves' tendency to be guided by the alpha wolf, the one with the highest fitness, to converge toward a better solution.

Through these behaviors and the population-based approach, the GWO algorithm efficiently explores the solution space, effectively balancing between exploration and exploitation. Consequently, GWO has demonstrated remarkable success in solving complex optimization problems and outperforming other metaheuristic algorithms¹⁴. The stages of GWO are detailed in Algorithm 2.

Algorithm2: Grey wolf optimizer's pseudocode¹⁴

1. Inputs: the values for N and T.
 2. Outputs: "X α "
-

Start by initializing the population of agents of search or grey wolves [X $_i$: $i = 1, 2, \dots, n$]

3. Set the maximum number of iterations as K. Set $t = 1$.
4. Calculate the fitness value for each search agent [g(X $_i$): $i = 1, 2, \dots, n$]

(The objective function being minimized is denoted as **g (X $_i$)**. This function represents the fitness value or performance measure associated with each individual search agent (grey wolf) represented by X $_i$ in the population)

5. Determine the best, second best, and third best search agents:

$$X\alpha = \text{Arg} (\min) [g (X_i) : i = 1 , 2 , \dots , n ,]$$

(X α (X Alpha): This variable represents the search agent (grey wolf) with the best fitness value (lowest g(X $_i$)) among all the individuals in the population. In other words, X α corresponds to the alpha (α) wolf, which is the global best solution found so far in the optimization process)

$$X\beta = \text{Arg} (\min) [g (X_i) : i = 1 , 2 , \dots , n , i \neq \alpha]$$

(X β (X Beta): X β represents the search agent (grey wolf) with the second-best fitness value (second lowest g(X $_i$)) in the population. It is the individual with the second-highest fitness level after X α . The X β corresponds to the beta (β) wolf, which helps in exploration and is used to diversify the search space)

$$X\delta = \text{Arg} (\min) [g (X_i) : i = 1 , 2 , \dots , n , i \neq \alpha , \beta]$$

(X δ (X Delta): X δ is the search agent (grey wolf) with the third-best fitness value (third lowest g(X $_i$)) among the population, excluding X α and X β . It is the individual with the third-highest fitness level and is used to further diversify the search space. X δ corresponds to the delta (δ) wolf)

6. Set $i = 1$ and let $a = 2(1 - t/K)$.
7. Pick six at random vectors $r1_j, r2_j, j = 1, 2, 3$, and compute:

$$A_j = a (2r1_j - 1) , C_j = 2r2_j , j = 1 , 2 , 3 .$$

$$D\alpha = | C1 . X\alpha - X_i | , D\beta = | C2 . X\beta - X_i | , D\delta = | C3 . X\delta - X_i | ,$$

$$X1 = X\alpha - A(1) . D\alpha , X2 = X\beta - A(2) . D\beta , X3 = X\delta - A(3) . D\delta$$

8. Update the search agents using (X $_i = X1 + X2 + X3$)/3.
 9. If $i < n$, increment i by 1, go to Step 4.
 10. If $t < K$, increment t by 1, go to Step 5.
 11. Put an end to the procedure using X α as the answer.
-

Glowworm Swarm Optimization algorithm (GSO)

It is a recently introduced algorithm in the field of swarm intelligence, inspired by the behavior of real glowworms. In this algorithm, each glowworm represents a potential solution to an optimization problem within a search space and carries a certain amount of "luciferin," which is a luminescent substance.

The movement of the glowworms is controlled by their proximity to luciferin, where the brighter the glowworm (higher luciferin intensity), the more favorable its position in the search space. Thus, the level of luciferin attached to each glowworm serves as an indicator of its fitness or quality of solution¹⁵. Glowworms employ a probabilistic technique to navigate toward neighboring glowworms within their local-decision area. They are attracted to those neighbors with higher luciferin intensity than their own, aiming to move towards better solutions to the optimization problem.

The decision radius and the size of the local-decision domain for each glowworm are influenced by the number of its neighbors. If the density of neighbors is low, the local-decision domain expands to search for more potential solutions. On the other hand, if the density of neighbors is high, the domain shrinks, enabling the swarm to divide into smaller

groups and explore different regions of the search space.

The effectiveness of the Glowworm Swarm Optimization algorithm has been demonstrated in various optimization problems. It has shown strong performance in finding near-optimal or even optimal solutions for complex, high-dimensional, and multi-modal optimization landscapes¹⁶. Successful applications of GSO include but are not limited to:

1. Wireless Sensor Network (WSN) Deployment: GSO has been employed to optimize the placement of sensor nodes in WSNs, ensuring efficient coverage and minimizing energy consumption.
2. Image Segmentation: GSO has been applied to image processing tasks, where it effectively identifies regions of interest and separates objects from the background.
3. Traveling Salesman Problem (TSP): GSO has shown promising results in solving the classic TSP, finding efficient routes for visiting a set of cities with minimum distance.
4. Function Optimization: GSO has been used to optimize complex mathematical functions, aiding in parameter tuning and finding global optima. Algorithm3 details the procedures involved in GSO.

Algorithm3 : Pseudocode of The Glowworm Swarm Optimization¹⁷

1. Generate a certain number of glowworms.
2. Make I the starting value for each glowworm's luciferin.
3. Direct the glowworm towards destination D.
4. **For** each glowworm ($1 \leq i \leq n$) upon reaching a vehicle,:
5. Calculate $D_i(t)$, $\pi_i(t)$.

$D_i(t)$: The distance measure from glowworm i to the destination D at iteration t . This measure helps the glowworms move towards the destination.

$\pi_i(t)$: A measure of the glow intensity of glowworm i at iteration t . It indicates how bright the glowworm appears to its neighbors, influencing their movement)

6. Use the equation: to update the luciferin.

$$l_i(t+1) \text{ is equal to } (1-p)l_i(t) + \gamma J(x_i(t+1)).$$

$(l_i(t+1))$: The updated luciferin value for glowworm i at iteration $t+1$. It is calculated based on the previous luciferin value $(l_i(t))$, a decay factor (p) , and a gain factor (γ) multiplied by the local neighborhood measure $(J(x_i(t+1)))$

$J(x_i(t+1))$: The light intensity of the location $x_i(t+1)$ where glowworm i intends to move to. It indicates how favorable that location is in terms of finding a better solution)

7. Choose the next-hop based on the probability equation:

$$P_{ij}(t) \text{ is equal to } \frac{l_j(t) - l_i(t)}{\sum_{k \in N_i(t)} l_k(t) - l_i(t)} .$$

$(P_{ij}(t))$: The probability that glowworm i chooses glowworm j as its next-hop neighbor at iteration t . It is determined based on the difference between their luciferin levels $(l_j(t) - l_i(t))$ and the sum of such differences within the neighborhood of glowworm i .

8. Move the glowworm i to the next hop.
9. **Repeat** steps 4 to 8 for all glowworms.
10. Node S transmits data to the neighbor with the highest luciferin.
11. **If** D be the receiving node:
12. The message to save the data.
13. Exit.
14. **Else**
15. Send the data to your neighbor who has the most luciferin.
16. Go back to step 11.

Below, Table 2 shows a comprehensive analysis describing the algorithms and identifying their strengths and weaknesses.

Table 2. Description of each algorithm with strengths and weaknesses for each one.

Algorithms	Description	Strengths	Weaknesses
1 GWO	GWO is inspired by the social hierarchy and hunting behavior of grey wolves. It mimics the hunting process of alpha, beta, and delta wolves to locate the optimal solution.	<ul style="list-style-type: none"> - Fast convergence: GWO often converges faster than some traditional optimization algorithms. - Global exploration: It can efficiently explore the search space, making it suitable for complex and multimodal optimization problems. - Easy implementation: GWO's simple structure allows for 	<ul style="list-style-type: none"> - Sensitivity to parameters: The performance of GWO can be sensitive to the choice of parameters, requiring careful tuning. - Premature convergence: It may converge prematurely to suboptimal solutions in certain scenarios. - Limited flexibility: GWO may not be as versatile as other optimization algorithms in

		straightforward implementation.	handling various types of optimization problems.
2 GSO	GSO is inspired by the bioluminescent behavior of glowworms and their communication through light emission. It is designed to optimize problems with spatially distributed solutions.	<ul style="list-style-type: none">- Adaptability to spatial problems: GSO is well-suited for problems involving spatially distributed solutions, making it potentially relevant for image-based tasks.- Efficient exploration: It can effectively explore the search space to locate promising solutions.- Scalability: GSO can be applied to large-scale optimization problems with a large number of variables.	<ul style="list-style-type: none">- Complexity: GSO may have a higher implementation complexity compared to some other optimization algorithms.- Sensitivity to parameters: Like GWO, parameter tuning is important to achieve good performance.- Lack of extensive applications: GSO is a relatively newer algorithm, and its application to various tasks, including image classification, may be limited.
3 MFO	MFO is a nature-inspired optimization algorithm based on the behavior of moths attracted to flames. It aims to find the optimal solution by simulating the movements of moths towards the brighter flame (better solutions).	<p>Simplicity: MFO is relatively easy to implement due to its straightforward concept.</p> <ul style="list-style-type: none">- Efficient for unimodal optimization: It performs well when the optimization problem has a single optimal solution.- Robustness: MFO is less likely to get stuck in local optima compared to gradient-based methods.	<ul style="list-style-type: none">- Slow convergence: MFO can converge slowly, especially for complex and multimodal optimization problems.- Lack of global exploration: It may struggle to explore the search space efficiently, leading to suboptimal solutions in complex scenarios.- Not widely studied: Compared to more established algorithms like Genetic Algorithms or Particle Swarm Optimization, MFO has limited research and application.

Preprocessing

The preprocessing stage of X-ray image enhancement is of paramount importance. X-ray images may suffer from noise, quality, and size issues due to equipment or photography technique-related factors. Therefore, the primary objective of this data preparation process is to facilitate feature extraction and enhance classification accuracy. In this paper, the Contrast Limited Adaptive Histogram Equalization (CLAHE) technique is employed to modify the image contrast, leveraging information from the image histograms. Prior to this, the images are denoised using the Gaussian blur filter.

By applying the CLAHE technique, the X-ray images are transformed into crisp and high-contrast representations. This transformation significantly improves the efficiency of the feature extraction procedure and subsequently enhances the accuracy of the classification process.

Furthermore, the CLAHE technique plays a pivotal role in addressing the challenges posed by diverse X-ray image qualities. By adaptively equalizing the image histogram, it ensures that the enhancement is performed on local regions rather than the entire image at once. This local contrast enhancement prevents the over-amplification of

noise and preserves the important details and structures in the X-ray images.

The denoising step preceding CLAHE is equally essential. The application of the Gaussian blur filter helps to suppress unwanted noise and artifacts present in the X-ray images. By reducing the noise, the subsequent CLAHE enhancement can work more effectively and produce better results.

The combination of denoising with the Gaussian blur filter and the adaptive contrast enhancement through CLAHE results in X-ray images that are not only visually pleasing but also highly amenable to feature extraction and classification algorithms. The enhancement process effectively highlights subtle patterns and structures that could be crucial for accurate medical diagnosis and analysis¹⁸.

As a result of this preprocessing stage, the X-ray images are transformed into a more standardized, informative, and feature-rich representation. This, in turn, significantly improves the performance of various image analysis tasks, such as disease detection, anomaly identification, and image-based diagnosis

Feature Extraction

The study focuses on extracting specific features from chest X-ray (CXR) images using the Gray Level Co-occurrence Matrix (GLCM) and Local Binary Pattern (LBP) methods. These techniques are employed to capture essential texture properties present in the images, aiding in their classification and analysis, the combination of GLCM and LBP methods enables the extraction of essential texture features from CXR images, leading to improved medical image classification accuracy¹⁹.

The GLCM method has been widely utilized in texture research and continues to be effective. It measures texture properties by analyzing the relationships between pixel values in an image. Six GLCM statistics are computed, namely angular second moment (ASM), variance, contrast, correlation (COR), homogeneity (HOM) and entropy. The GLCM matrix connects the distance and angle between pixels in the image, providing information about the grayscale values' co-

occurrence in each of the four different orientations used (0, 45, 90, and 135).

The LBP feature extraction technique represents the image for classification purposes by extracting numerical features²⁰. CXR images contain texture due to the recurring patterns, indicating how the chest images were formed based on the absorption of different spectrums dependent on tissue density.

The LBP approach follows specific equations (Eq. 1 to Eq. 8) to generate the feature set:

$$LBP = \sum_{n=0}^7 s(I_n - I_c) \times 2^n \quad 1$$

Eq. 1 calculates the LBP value for a pixel using the sum of differences between its neighbors and the center pixel.

$$A_{i,j}^1 = S(I_1, I_c) \times 2^7 + S(I_2, I_c) \times 2^6 \quad 2$$

$$A_{i,j}^2 = S(I_3, I_c) \times 2^5 + S(I_4, I_c) \times 2^4 \quad 3$$

$$A_{i,j}^3 = S(I_5, I_c) \times 2^3 + S(I_6, I_c) \times 2^2 \quad 4$$

$$A_{i,j}^4 = S(I_7, I_c) \times 2^1 + S(I_8, I_c) \times 2^0 \quad 5$$

Eq. 2 to Eq. 5 compute four different texture patterns ($A_{i,j}^1$ to $A_{i,j}^4$) by comparing the center pixel to its eight neighbors in a circular pattern.

$$A = A_{i,j}^1 + A_{i,j}^2 + A_{i,j}^3 + A_{i,j}^4 \quad 6$$

Eq. 6 aggregates the four texture patterns ($A_{i,j}^1$ to $A_{i,j}^4$) into a single value, A.

$$LBP = \text{Histogram}_A \quad 7$$

Eq. 7 creates the histogram of the aggregated texture patterns (A) for each cell in the image.

$$S(z) = \begin{cases} 0, & z < 0 \\ 1, & z \geq 0 \end{cases} \quad 8$$

Eq. 8 is a step function that returns 1 if the argument is non-negative and 0 otherwise.

Show the importance of equations, I_c represents the pixel value in the center, and I_n represents the pixel values of the neighbors. The LBP operator generates bits (z) based on the difference between the center pixel and its adjacent pixels. The resulting LBP value, along with the texture patterns

$(A_{i,j}^1$ to $A_{i,j}^4$), is utilized to capture distinct texture information from the CXR images. Fig. 2 shows the LBP operator's pixel labeling technique.

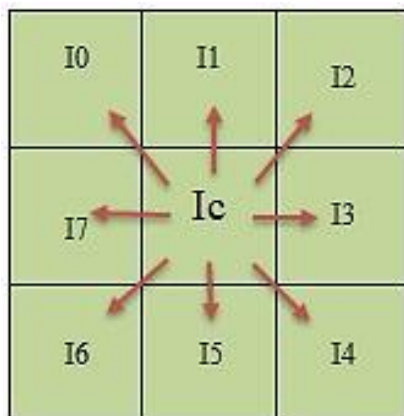


Figure 2. The LBP operator labeling pixels.

Feature Selection

The feature selection process for medical image classification is a critical step as it significantly impacts the precision and effectiveness of the classification model. In this study, three swarm intelligence wrapping methods were employed for feature selection: Moth-Flame Optimization algorithm (MFO), Glowworm Swarm Optimization algorithm (GSO), and Grey wolf optimizer algorithm (GWO).

(MFO), (GSO), and (GWO) are powerful metaheuristic optimization techniques that mimic the collective behavior of swarms and wolf packs to efficiently search for optimal solutions.

In the feature selection process, the classification method was treated as a "black box," meaning that its internal workings were not explicitly considered. Instead, the performance of the classification method was solely used as an indicator to evaluate different feature subsets and guide the search.

Criteria and Metrics for Evaluation:

To assess the quality of different feature subsets, several criteria and metrics were employed. These metrics are essential for guiding the swarm intelligence algorithms in selecting the most informative features. The following criteria were used:

1. Classification Accuracy: The accuracy of the classification model was measured using standard performance metrics such as precision, recall, F1-score, and overall accuracy. These metrics reflect the ability of the model to correctly classify medical images.

2. Feature Subset Size: The number of selected features was also considered as a criterion. The goal was to find the optimal trade-off between the size of the feature subset and the classification performance. Too few features might result in underfitting, while too many could lead to overfitting.

3. Feature Importance: The importance of each feature in the classification process was assessed. Features that contributed significantly to the model's performance were given higher importance scores.

Throughout the feature selection process, the swarm intelligence algorithms (MFO, GSO, and GWO) dynamically adjusted their search strategies based on performance metrics. The algorithms explored different combinations of features and prioritized those subsets that exhibited higher classification accuracy and smaller feature subset sizes. Additionally, the algorithms utilized the feature importance scores to focus on the most informative features.

By incorporating these criteria and metrics into the swarm intelligence algorithms, the feature selection process effectively identified the most relevant features for medical image classification, leading to improved model accuracy and generalization capabilities.

Classifiers

The basic purpose of classification is to assign a classification to innovative specimens that have not, yet, been assigned to a certain class. Hence, the proposed system must first train the classifier to detect the data's characteristics as well as the relationship between the class label and the attribute values, these classifiers provide distinct methods, properties, and performance, which make them valuable tools in various classification tasks. In this sense, three classifiers were explained within the approach of this study:

Support Vector Machine (SVM)

SVM is a powerful supervised machine learning technique used for both regression and classification tasks. The implementation involves the following steps:

- Kernel Function: SVM aims to find the optimal hyperplane in the N-dimensional feature space for classification. For linearly separable data, a linear kernel function is commonly used. However, for data with higher nonlinearity, nonlinear kernels such as Radial Basis Function (RBF) kernels are employed²¹
- Regularization Parameter: The regularization parameter (C) controls the trade-off between maximizing the margin and minimizing the classification errors on the training data.
- Soft Margin: SVM allows for soft margins, which permit some misclassifications in favor of a more generalized model. The soft margin parameter (C) influences the balance between margin size and misclassification tolerance²².

K - Nearest Neighbor (KNN)

KNN is a simple and effective classification algorithm that sorts items into groups based on their proximity to a given object. The implementation involves the following steps:

- Parameter: 'k' represents the number of nearest neighbors to consider during classification. It is essential to choose an appropriate value for 'k' to ensure accurate predictions.
- Distance Metric: The Euclidean distance is commonly used to measure the proximity between data points in feature space.
- Classification: To classify a new data point, the algorithm finds the 'k' closest data points from the training set and assigns the class label based on the majority class among these neighbors^{23 24}.

Extreme Gradient Boosting (XGboost)

XGboost is a powerful gradient boosting algorithm known for its superior performance and fast execution speed. The implementation involves the following aspects:

- Parameters: XGboost offers a wide range of parameters to tune for optimal performance. Some of the key parameters include the number of boosting rounds (n_estimators), maximum tree depth (max_depth), learning rate (eta), and subsample ratio (subsample).
- Parallel Computation: XGboost employs parallel computation to build trees across all CPUs during training, which significantly speeds up the process.
- Tree Pruning: Instead of traditional stopping criteria, XGboost uses the 'max depth' parameter for tree pruning, which contributes to improved model generalization²⁵.

Performance Evaluation

In this study, the performance of the COVID-19 detection system was evaluated using two distinct datasets: the "Moderate Dataset: comprises 400 chest X-ray images of confirmed COVID-19 infection and an equal number of 400 uninfected chest X-ray images." and the "Big Dataset: it consists of 5,500 normal chest X-ray images and 4,044 images with confirmed cases of COVID-19 infection".

Before training the categorization model, standard preprocessing steps were applied to both datasets to ensure data uniformity and compatibility. These steps included resizing the images to a consistent resolution, denoising, and contrast correlation.

The findings from this evaluation may have significant implications for the field of medical image analysis and COVID-19 diagnosis. High accuracy and F1-score would indicate the model's effectiveness in detecting COVID-19 cases, while high precision and recall would demonstrate the system's ability to minimize false positives and false negatives, respectively. Such a robust COVID-19 detection system could prove instrumental in supporting healthcare professionals and enhancing patient care during the ongoing pandemic.

to assess the performance of the COVID-19 detection system, the following evaluation metrics were utilized:

Accuracy (ACC)

The accuracy measure is a ratio of the proportion of right predictions to the total number

of instances that were analyzed. One method to calculate it is to use the equation shown below Eq. 9.

$$\text{Accuracy} = (\text{TP} + \text{TN}) / (\text{TP} + \text{TN} + \text{FP} + \text{FN}) \quad 9$$

Precision

This measure contrasts the proportion of accurate detections to all positive detections. The equation below Eq.10 might be used to compute it:

$$\text{Precision} = \text{TP} / (\text{TP} + \text{FP}) \quad 10$$

Recall/Sensitivity

This is calculated by dividing the total number of correctly predicted positive outcomes by the total number of positive cases. The following equation Eq. 11 could be used to determine this metric:

$$\text{Recall} = \text{TP} / (\text{TP} + \text{FN}) \quad 11$$

Specificity

Specificity, often known as the true negative rate (TNR), is a numerical scale that assesses how well a

binary classification test is able to detect negative conditions correctly. It might be calculated using the following equation Eq. 12:

$$\text{Specificity} = \text{TN} / (\text{TN} + \text{FP}) \quad 12$$

F1 - score

When calculating the weighted harmonic mean, recall and accuracy are taken into account. It might be calculated using the following equation Eq. 13:

$$\text{F1} = 2 \times (\text{Specificity} \times \text{Recall}) / (\text{Specificity} + \text{Recall}) \quad 13$$

where "TP" refers to "true positives," or positive images with precise classifier labels, and "TN" refers to "true negatives," or negative images with correct classifier labels. False positives (FP) are positive photos that were incorrectly categorized as negatives, whereas false negative (FN) are the opposite: negative images that were incorrectly categorized as positive.^{26 27}

Results and Discussion

In this research, three different algorithms were compared. Individuals with and without Coronavirus (COVID-19) infections were distinguished and compared using the CXR dataset. Several swarm intelligence algorithms, including XGboost, SVM, and KNN classifiers, were utilized to assess the performance of feature selection strategies in swarm algorithms. Table 3 presents the performance of the MFO feature selection algorithm which achieves 99%, 86% and 98% for small data, and achieves 96 %, 80% and 93% for big data across three classifiers: XGboost, SVM and KNN. Table 4, on the other hand, presents the performance of the GWO feature selection algorithm, which achieves 99%, 90% and 99% for small data, and 95%, 89% and 90% for big data across three classifiers XGboost, SVM and KNN. Table 5 shows the performance of the GSO method used in characteristic selection, which for small data achieves 99% and 72% and 99% and for big data achieves 97% and 75% and 92% on three classifiers (KNN, SVM, and XGboost), The table 6 shows a comparison of the final results of the two data sets for the three algorithms.

The implications of these results are highly significant for medical imaging applications, especially in the context of COVID-19 diagnosis. The ability of these algorithms to accurately distinguish COVID-19 infections from non-infected cases can greatly aid healthcare professionals in the early detection and prompt treatment of the disease. Moreover, the use of swarm intelligence algorithms, as demonstrated in this research, holds promise for enhancing the efficiency and effectiveness of feature selection strategies, thus contributing to improved diagnostic accuracy.

The potential applications of the findings are extensive. These algorithms can be integrated into existing medical imaging systems to assist radiologists in their decision-making process and improve the overall diagnostic accuracy of COVID-19 cases. Furthermore, the research provides valuable insights into the use of swarm intelligence techniques for medical image analysis, which could inspire further research and development in this domain.

Table 3. MFO performance over XGboost, KNN, and SVM classifiers.

	Algo.	Precision	Recall	F1-score	ACC
Small data	XGBoost	0.96	0.94	0.96	0.99854
	SVM	0.90	0.85	0.86	0.86666
	k-NN	0.97	0.99	0.98	0.98000
Big data	XGBoost	0.93	0.94	0.91	0.96873
	SVM	0.85	0.78	0.79	0.80979
	k-NN	0.92	0.91	0.91	0.92000

Table 4. GWO performance over XGboost, KNN, and SVM classifiers.

	Algo.	Precision	Recall	F1-score	ACC
Small data	XGBoost	0.99	0.98	0.99	0.99840
	SVM	0.84	0.98	0.91	0.90833
	k-NN	0.98	0.99	0.99	0.99000
Big data	XGBoost	0.91	0.90	0.90	0.95939
	SVM	0.89	0.90	0.89	0.89650
	k-NN	0.90	0.89	0.91	0.90000

Table 5. GSO performance over XGboost, KNN, and SVM classifiers.

	Algo.	Precision	Recall	F1-score	ACC
Small data	XGBoost	0.97	0.98	0.97	0.99777
	SVM	0.82	0.71	0.70	0.72916
	k-NN	0.97	0.98	0.99	0.99000
Big data	XGBoost	0.92	0.93	0.92	0.97012
	SVM	0.82	0.71	0.71	0.75559
	k-NN	0.92	0.91	0.91	0.92000

Table 6. Comparison of the results of the two data sets for the three algorithms.

	Algorithms	Dataset	XGboost	KNN	SVM
1	GWO	Small Dataset	0.99840	0.99000	0.90833
		Big Dataset	0.95939	0.90000	0.89650
2	GSO	Small Dataset	0.99777	0.99000	0.72916
		Big Dataset	0.97012	0.92000	0.75559
3	MFO	Small Dataset	0.99854	0.98000	0.86666
		Big Dataset	0.96873	0.92000	0.80979

The above tables indicate that KNN and XGBoost classifiers outperformed SVM classifiers in terms of classification accuracy when utilizing MFO, GWO, and GSO algorithms as feature selection techniques. On the other hand, the SVM classifier yielded a comparatively lower classification rate.

The figures below (Fig. 3, Fig. 4, and Fig. 5) show the ratio of the accuracy, precision, recall, and F1 values for all algorithms.

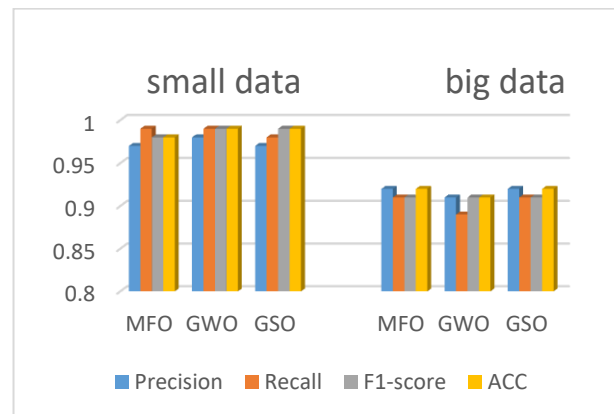


Figure 3. The accuracy, precision, recall, and the F1 values for all algorithms over KNN classifier



Figure 4.The accuracy, precision, recall, and the F1 values for all algorithms over SVM classifier

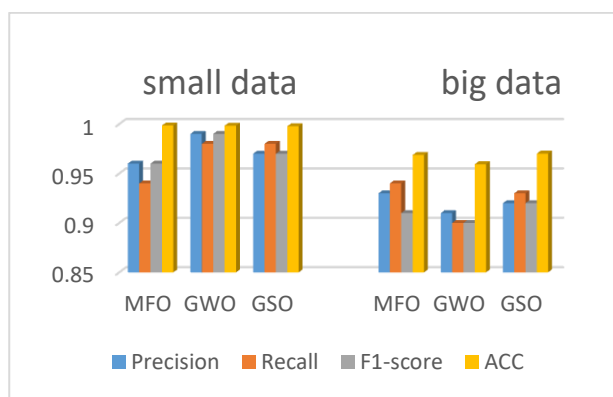


Figure 5. The accuracy, precision, recall, and the F1 values for all algorithms over XGboost classifier

Dataset

In most instances, using the right data set is crucial when assessing COVID-19 detection

Conclusion

In order to distinguish COVID-19 patients with infections from regular CXR images, this study employed various swarm intelligence algorithms and multiple chest X-ray classifiers, utilizing two databases. The findings showed that the big data group's highest level of accuracy came from the XGBoost and KNN techniques of 97%, whereas the SVM techniques recorded the lowest accuracy at 89%. In the small data group, XGBoost and KNN classifiers achieved the highest accuracy rates up to 99%, while SVM technologies revealed the lowest accuracy rates at 90%. This study's key findings showcase the potential of swarm intelligence

systems. Two different datasets that were used to train the categorization model are described in the articles below:

The moderate dataset includes 400 chest X-rays with confirmed COVID-19 infection and 400 uninfected chest X-rays. Both image collections were obtained from Kaggle²⁸. The photographs included in this dataset were saved as PNG files with a grayscale scale.

The Big Dataset is derived from Mendeleey Data²⁹ and consists of 5,500 normal chest X-ray images and 4,044 images with confirmed cases of COVID-19 infection. The photographs included in this collection were saved in JPEG, JPG, and PNG file formats, each with a grayscale-level scale.

Chest X-ray images (anterior-posterior) were selected from retrospective cohorts of pediatric patients one to five years old from Guangzhou Women and Children's Medical Center, Guangzhou. All chest X-ray imaging was performed as part of patients' routine clinical care.

For the analysis of chest x-ray images, all chest radiographs were initially screened for quality control by removing all low quality or unreadable scans. The diagnoses for the images were then graded by two expert physicians before being cleared for training to the AI system. In order to account for any grading errors, the evaluation set was also checked by a third expert.

algorithms and chest X-ray classifiers in distinguishing COVID-19 patients from regular CXR images. However, to advance the field further, future research should focus on extraction of other feature sets could be experimentally tested into our proposed classification schema. Additionally, Future research should consider integrating other diagnostic modalities, such as CT scans or molecular testing, to enhance the accuracy and reliability of COVID-19 detection systems, explore the potential of the proposed algorithms in distinguishing COVID-19 from other respiratory

conditions that may exhibit similar symptoms on chest X-rays.

Authors' Declaration

- Conflicts of Interest: None.
- We hereby confirm that all the Figures and Tables in the manuscript are ours. Furthermore, any Figures and images, that are not ours, have been included with the necessary permission for re-publication, which is attached to the manuscript.
- Ethical Clearance: The project was approved by the local ethical committee in University of Babylon. Obtaining informed consent from relevant stakeholders poses challenges for researchers in accurately identifying individuals.

Authors' Contribution Statement

A.M. , H.A. and Y.H. Contributed to the research analysis, design, implementation of the research, analysis of the results, and the writing of the manuscript.

References

1. Ali RH, Abdulsalam WH. The Prediction of COVID 19 Disease Using Feature Selection Techniques. J Phys Conf Ser. 2021; 1879(2): 1-13. <https://doi.org/10.1088/1742-6596/1879/2/022083>
2. Huang C, Wang Y, Li X, et al. Clinical features of patients infected with 2019 novel coronavirus in Wuhan, China. Lancet. 2020; 395(10223): 497-506. [https://doi.org/10.1016/S0140-6736\(20\)30183-5](https://doi.org/10.1016/S0140-6736(20)30183-5)
3. Songram P, Chomphuwiset P, Kawattikul K, Jareanpon C. Classification of chest X-ray images using a hybrid deep learning method. Indones J Electr Eng Comput Sci. 2022; 25(2): 867-874. <https://doi.org/10.11591/ijeecs.v25.i2.pp867-874>
4. Narin A, Kaya C, Pamuk Z. Automatic detection of coronavirus disease (COVID-19) using X-ray images and deep convolutional neural networks. Pattern Anal Appl. 2021; 24(3): 1207-1220. <https://doi.org/10.1007/s10044-021-00984-y>
5. Antin B, Kravitz J, Martayan E. Detecting Pneumonia in Chest X-Rays with Supervised Learning. Semant org. 2017; (46632050): 1-5. <http://cs229.stanford.edu/proj2017/final-reports/5231221.pdf>
6. Liang G, Zheng L. A transfer learning method with deep residual network for pediatric pneumonia diagnosis. Elsevier. 2020; 187: 1-9. <https://doi.org/10.1016/j.cmpb.2019.06.023>
7. Sethy PK, Behera SK, Ratha PK, Biswas P. Detection of coronavirus disease (COVID-19) based on deep features and support vector machine. Int J Math Eng Manag Sci. 2020; 5(4): 643-651. <https://doi.org/10.20944/preprints202003.0300.v1>
8. Mohammed SN, Alkinani FS, Hassan YA. Automatic computer aided diagnostic for COVID-19 based on chest X-Ray image and particle swarm intelligence. Int J Intell Eng Syst. 2020; 13(5): 63-73. <https://doi.org/10.22266/ijies2020.1031.07>
9. Too J, Mirjalili S. A Hyper Learning Binary Dragonfly Algorithm for Feature Selection: A COVID-19 Case Study. Knowl Based Syst. 2021; 212: 1-29. <https://doi.org/10.1016/j.knosys.2020.106553>
10. Bezdán T, Cvetnic D, Gajic L, Zivkovic M, Strumberger I, Bacanin N. Feature Selection by Firefly Algorithm with Improved Initialization Strategy. ACM Int Conf Proceeding Ser. 2021; 8: 1-8. <https://doi.org/10.1145/3459960.3459974>
11. Zou L, Zhou S, Li X. An Efficient Improved Greedy Harris Hawks Optimizer and Its Application to Feature Selection. Entropy. 2022; 24(8): 1-22. <https://doi.org/10.3390/e24081065>
12. Issa AS, Ali YH. Comparative Analysis of Swarm Algorithms to Classification of covid19 on X-Rays. 2022 Int Conf Data Sci Intell Comput. 2022; 22883321(Icdsic): 164-169. <https://doi.org/10.1109/ICDSIC56987.2022.10075733>
13. Sahoo SK, Saha AK, Ezugwu AE, Agushaka J O, Abuhaija B, Alsoud A R, et al. Moth Flame Optimization: Theory, Modifications, Hybridizations, and Applications. Arch Comput Methods Eng. 2023; 30(1): 391-426. <https://doi.org/10.1007/s11831-022-09801-z>
14. Mirjalili S, Mirjalili SM, Lewis A. Grey Wolf Optimizer. Adv Eng Softw. 2014; 69: 46-61. <https://doi.org/10.1016/j.advengsoft.2013.12.007>
15. Zainal N, Zain A, Radzi N, Udin A. Glowworm Swarm Optimization (GSO) Algorithm for

- Optimization Problems: A State-of-the-Art Review. *Appl Mech Mater.* 2013; 421: 507-511. <https://doi.org/10.4028/www.scientific.net/AMM.421.507>
16. Mazher AN, Waleed J. Retina based glowworm swarm optimization for random cryptographic key generation. *Baghdad Sci J.* 2022; 19(1): 179-188. <https://doi.org/10.21123/BSJ.2022.19.1.0179>
17. Yarinezhad R, Sarabi A. New Routing Algorithm for Vehicular Ad-hoc Networks based on Glowworm Swarm Optimization Algorithm. *J artif intel data min.* 2019; 7(1): 69-76. <https://doi.org/10.22044/JADM.2018.6516.1765>
18. Stimper V, Bauer S, Ernstorfer R, Schölkopf B, Xian RP. Multidimensional Contrast Limited Adaptive Histogram Equalization. *IEEE Access.* 2019; 7: 165437-165447. <https://doi.org/10.1109/ACCESS.2019.2952899>
19. Al Okashi OM, Ahmed IT, Abed LH. COVID-19 detection based on combined domain features. *Indones J Electr Eng Comput Sci.* 2022; 26(2): 965-973. <https://doi.org/10.11591/ijeecs.v26.i2.pp965-973>
20. Vigneshl T, Thyagarajan KK. Local binary pattern texture feature for satellite imagery classification. *Int Conf Sci Eng Manag.* 2014; 32331: 1-6. <https://doi.org/10.1109/ICSEMR.2014.7043591>
21. Battur R, Narayana J. Classification of medical X-ray images using supervised and unsupervised learning approaches. *Indones J Electr Eng Comput Sci.* 2023; 30(3): 1713-1721. <https://doi.org/10.11591/ijeecs.v30.i3.pp1713-1721>
22. Eds DA jumeily. *Emerging Technology Trends in Internet of Things and Computing.* springer; 2021. <https://doi.org/10.1007/978-3-030-97255-4>
23. Samsir S, Sitorus JHP, Ritonga Z, Aini F. Comparison of machine learning algorithms for chest X-ray image COVID-19 classification. 2021; 012040: 1-7. <https://doi.org/10.1088/1742-6596/1933/1/012040>
24. Mohamed Ali SS, Alsaedi AH, Al-Shammary D, Alsaedi HH, Abid HW. Efficient intelligent system for diagnosis pneumonia (SARSCoVID19) in X-ray images empowered with initial clustering. *Indones J Electr Eng Comput Sci.* 2021; 22(1): 241-251. <https://doi.org/10.11591/ijeecs.v22.i1.pp241-251>
25. Ali ZA, Abduljabbar ZH, Taher HA, Sallow AB, Almufti SM. Exploring the Power of eXtreme Gradient Boosting Algorithm in Machine Learning : a Review. *Acad J Nawroz Univ.* 2023; 12(2): 320-15. <https://doi.org/10.25007/ajnu.v12n2a1612>
26. Sahlol AT, Yousri D, Ewees AA, Al MAA. OPEN COVID - 19 image classification using deep features and fractional - order marine predators algorithm. *Sci Rep.* 2020; 10: 15364: 1-15. <https://doi.org/10.1038/s41598-020-71294-2>
27. Abdullah TH, Alizadeh F, Abdullah BH. COVID-19 Diagnosis System using SimpNet Deep Model. *Baghdad Sci J.* 2022; 19(5): 1078-1089. <https://doi.org/10.21123/bsj.2022.6074>
28. Kaggle. Chest X-Ray Images (Pneumonia) | Kaggle. Kaggle's chest X-ray images (Pneumonia) dataset. Published 2020. <https://www.kaggle.com/datasets/paultimothymooney/chest-xray-pneumonia>
29. El-Shafai W, E. Abd El-Samie F. Extensive COVID-19 X-Ray and CT Chest Images Dataset. *Mendeley Data.* Published online 2020. <https://data.mendeley.com/datasets/8h65ywd2jr/3>

تحليل مقارنة لـ MFO و GWO و GSO لتصنيف صور الأشعة السينية للصدر Covid-19

اسراء محسن محمد¹، حسين عطية لفتة²، يسرى حسين علي³

¹قسم علوم الحاسوب، كلية العلوم للبنات، جامعة بابل، بابل، العراق.

²قسم علوم الحاسوب، كلية العلوم للبنات، جامعة بابل، بابل، العراق.

³قسم علوم الحاسوب، الجامعة التكنولوجية، بغداد، العراق.

الخلاصة

تلعب الصور الطبية دورًا حاسمًا في تصنيف الأمراض والحالات المختلفة. إحدى طرق التصوير هي الأشعة السينية التي توفر معلومات بصرية قيمة تساعد في تحديد وتوصيف مختلف الحالات الطبية. لطالما استخدمت الصور الشعاعية للصدر (CXR) لفحص ومراقبة العديد من اضطرابات الرئة، مثل السل والالتهاب الرئوي وانخماص الرئة والفتق. يمكن الكشف عن COVID-19 باستخدام صور CXR أيضًا. تم اكتشاف COVID-19، وهو فيروس يسبب التهابات في الرئتين والممرات الهوائية في الجهاز التنفسي العلوي، لأول مرة في عام 2019 في مقاطعة ووهان بالصين، ومنذ ذلك الحين يُعتقد أنه يتسبب في تلف كبير في مجرى الهواء، مما يؤثر بشدة على رئة الأشخاص المصابين. انتشر الفيروس بسرعة في جميع أنحاء العالم، وتم تسجيل الكثير من الوفيات والحالات المتزايدة بشكل يومي. يمكن استخدام CXR لمراقبة آثار COVID-19 على أنسجة الرئة. تبحث هذه الدراسة في تحليل مقارنة لأقرب جيران (KNN) k، و Extreme Gradient Boosting (XGboost)، و Support-Vector Machine (SVM)، وهي بعض مناهج التصنيف لاختيار الميزات في هذا المجال باستخدام خوارزمية Moth-Flame Optimization (MFO)، وخوارزمية Gray Wolf Optimizer (GWO)، وخوارزمية Glowworm Swarm Optimization (GSO). في هذه الدراسة، استخدم الباحثون مجموعة بيانات تتكون من مجموعتين على النحو التالي: 9544 صورة بالأشعة السينية ثنائية الأبعاد، والتي تم تصنيفها إلى مجموعتين باستخدام اختبارات التحقق من صحتها: 5500 صورة لرئتين سليمتين و4044 صورة للرئتين مع COVID-19. تتضمن المجموعة الثانية 800 صورة و400 صورة لرئتين سليمتين و400 رئة مصابة بـ COVID-19. تم تغيير حجم كل صورة إلى 200 × 200 بكسل. كانت الدقة والاستدعاء ودرجة F1 من بين معايير التقييم الكمي المستخدمة في هذه الدراسة.

الكلمات المفتاحية: التصنيف، COVID-19، (XGboost)، خوارزمية تحسين لهب العثة (MFO)، خوارزمية تحسين الذئب الرمادي (GWO)، خوارزمية تحسين دودة التوهج (GSO).